

Design of a Bioactive Small Molecule That Targets the Myotonic Dystrophy Type 1 RNA via an RNA Motif–Ligand Database and Chemical Similarity Searching

Raman Parkesh,^{†,‡} Jessica L. Childs-Disney,^{†,‡} Masayuki Nakamori,[‡] Amit Kumar,[†] Eric Wang,[§] Thomas Wang,[§] Jason Hoskins,[‡] Tuan Tran,[†] David Housman,[§] Charles A. Thornton,[‡] and Matthew D. Disney^{*,†}

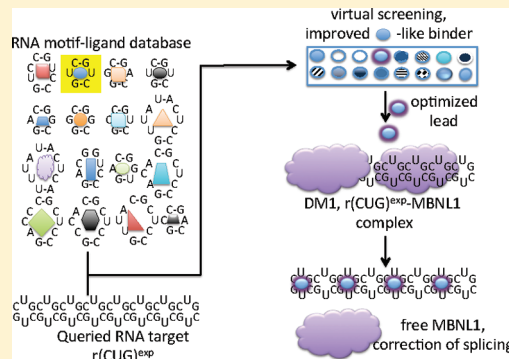
[†]Department of Chemistry, Scripps Florida, 130 Scripps Way, Jupiter, Florida 33458, United States

[‡]Department of Neurology, University of Rochester, Rochester, New York 14642, United States

[§]Department of Biology, Massachusetts Institute of Technology, 31 Ames Street, 68-132, Cambridge, Massachusetts 02139, United States

S Supporting Information

ABSTRACT: Myotonic dystrophy type 1 (DM1) is a triplet repeating disorder caused by expanded CTG repeats in the 3'-untranslated region of the dystrophin myotonia protein kinase (*DMPK*) gene. The transcribed repeats fold into an RNA hairpin with multiple copies of a 5'CUG/3'GUC motif that binds the RNA splicing regulator muscleblind-like 1 protein (MBNL1). Sequestration of MBNL1 by expanded r(CUG) repeats causes splicing defects in a subset of pre-mRNAs including the insulin receptor, the muscle-specific chloride ion channel, sarco(endo)plasmic reticulum Ca²⁺ ATPase 1, and cardiac troponin T. Based on these observations, the development of small-molecule ligands that target specifically expanded DM1 repeats could be of use as therapeutics. In the present study, chemical similarity searching was employed to improve the efficacy of pentamidine and Hoechst 33258 ligands that have been shown previously to target the DM1 triplet repeat. A series of in vitro inhibitors of the RNA–protein complex were identified with low micromolar IC₅₀'s, which are >20-fold more potent than the query compounds. Importantly, a bis-benzimidazole identified from the Hoechst query improves DM1-associated pre-mRNA splicing defects in cell and mouse models of DM1 (when dosed with 1 mM and 100 mg/kg, respectively). Since Hoechst 33258 was identified as a DM1 binder through analysis of an RNA motif–ligand database, these studies suggest that lead ligands targeting RNA with improved biological activity can be identified by using a synergistic approach that combines analysis of known RNA–ligand interactions with chemical similarity searching.



INTRODUCTION

RNA plays important roles in biological processes. For example, RNA splicing patterns control the protein isoforms derived from a single primary transcript, and microRNAs regulate processes such as developmental timing by controlling the lifetime of an mRNA.^{1–5} RNA-mediated diseases^{6–11} can be caused by an RNA loss-of-function or a gain-of-function. RNA gain-of-function causes or contributes to triplet and tetra-repeating disorders such as the myotonic dystrophies,^{12–14} Huntington's disease,¹⁵ spinocerebellar ataxia,^{16,17} and fragile X syndrome.¹⁸ In myotonic dystrophy type 1 (DM1), an expanded rCUG repeat in the 3'-untranslated region (UTR) of the dystrophin myotonia protein kinase (*DMPK*) mRNA binds and inactivates muscleblind-like 1 protein (MBNL1).^{19–22} Sequestration of MBNL1 by the expanded repeats results in the mis-splicing of a subset of pre-mRNAs including the muscle-specific chloride ion channel²³ and the insulin receptor (IR)^{24–26} among others.^{27,28} Splicing defects in

the chloride ion channel and the IR pre-mRNAs explain the myotonia and insulin insensitivity, respectively, associated with myotonic dystrophy. The presence of expanded rCUG repeats also causes reduction in the nucleocytoplasmic transport of the *DMPK* mRNA and thus the expression level of *DMPK*.^{21,29} Reduced transport occurs because the expanded repeats bind to various proteins and form nuclear foci.^{22,30–35}

The disease model in which expanded rCUG repeats bind and inactivate MBNL1 points to a therapeutic strategy in which a small molecule or oligonucleotide binds the repeats and frees MBNL1. This therapeutic avenue is supported by several studies,^{36–39} including the correction of splicing defects by overexpression of MBNL1.²⁰ Several groups have identified small molecules that inhibit the rCUG-MBNL1 interaction, including a Hoechst derivative,⁴⁰ an aminoglycoside deriva-

Received: November 5, 2011

Published: February 2, 2012

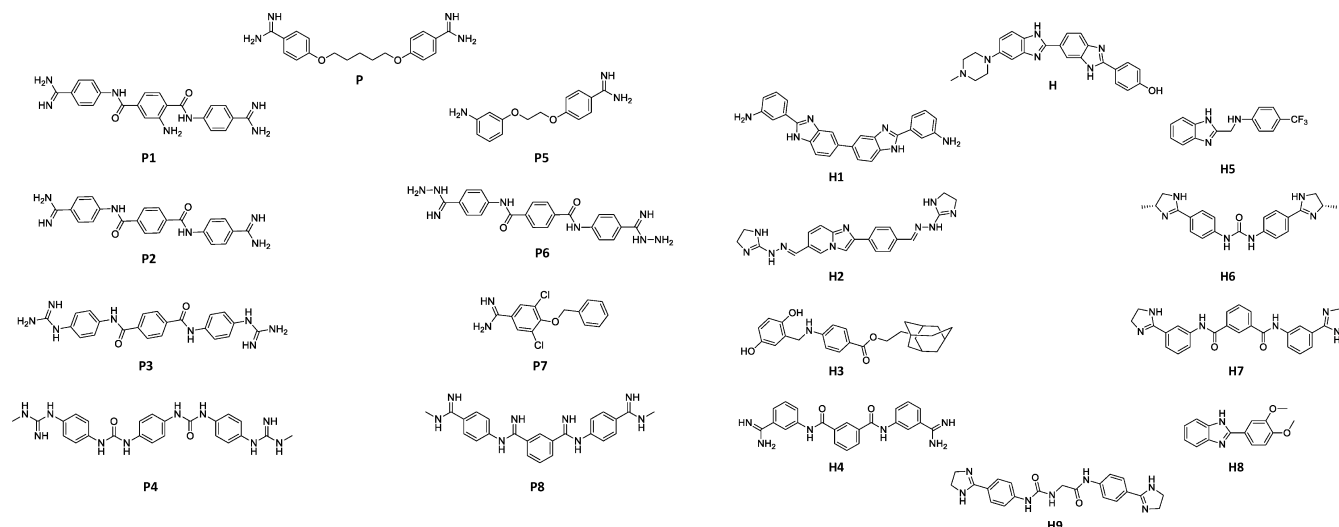


Figure 1. Structures of the most potent lead compounds that inhibit formation of the r(CUG)₁₂-MBNL1 complex. The compounds were identified from chemical similarity searching in which pentamidine (P) and Hoechst 33258 (H) were used as query molecules. Left, the most potent pentamidine-like compounds; right, the most potent Hoechst 33258-like compounds.

tive,⁴¹ an acridine–triazole conjugate,⁴² pentamidine,³⁸ and peptides and derivatives thereof.^{36,43} Pentamidine³⁸ and oligonucleotides^{37,39} improve splicing defects in cell culture and animal models.

It is likely that the small molecules that inhibit the rCUG-MBNL1 interaction represent privileged scaffolds for binding rCUG repeats. Therefore, we used Hoechst 33258 and pentamidine as query molecules to identify potential lead ligands with improved potencies and biological activity in the National Cancer Institute (NCI) and eMolecules databases; that is, we identified the small molecules that are similar in shape and/or the positioning of functional groups, rings, hydrophobic groups, charge, etc. Once identified, the potencies of the compounds were tested in an *in vitro* assay. Many ligands are more potent than the parent pentamidine and Hoechst 33258 compounds; the five most potent compounds showed a >20- to >100-fold improvement for disruption of the rCUG-MBNL1 complex. A bis-benzimidazole, which was identified by the Hoechst query, improves DM1-associated pre-mRNA splicing defects in cellular and animal models. Since Hoechst 33258 was identified to bind the repeating 5'CUG/3'GUC motif in the DM1 RNA using an RNA motif–ligand database, these studies suggest that the database approach can be useful to identify lead ligands targeting RNA that can be further improved by using chemical similarity searching.

RESULTS AND DISCUSSION

Previous reports have shown that small molecules^{40–43} and oligonucleotides³⁹ can disrupt formation of the toxic RNA–protein interaction that causes myotonic dystrophy *in vitro*. Two of these small molecules, Hoechst 33258 (H) and pentamidine (P) (Figure 1), are interesting lead ligands that are amenable to chemical similarity searching. Hoechst 33258 was identified as a lead ligand by analysis of an RNA motif–ligand database,^{40,44} while pentamidine was identified from a previous report.³⁸ The goal of chemical similarity searching is to identify compounds with similar shapes or positioning of functional groups that have improved biological activity and/or improved pharmacodynamic or pharmacokinetic properties.

Chemical Similarity Searching Methodology. Hoechst 33258 (H) and pentamidine (P) (Figure 1) were used as query molecules to identify compounds in the NCI and eMolecules databases that are similar in shape and/or structure. The NCI database was used because it is an easily accessible, medium-sized database (250,000 compounds). It contains the most complete collection of compounds that represents broad chemical space, and the compounds are available free of charge for academic purposes. All compounds used for virtual screening in the NCI database have complete stereochemistry specification, allowing reliable 3D coordinates of stereoisomers to be calculated. The eMolecules database (8,000,000 compounds) was used as it contains the most comprehensive, commercially available collection of small molecules for virtual screening.

Pentamidine and Hoechst 33258 are attractive lead compounds for virtual screening because of their relative structural simplicity, which leads to computationally less demanding 3D shape comparison. Three-dimensional computational shape comparison was completed using the 3D alignment software Rapid Overlay of Chemical Structure (ROCS) because of its fast and efficient implementation of a 3D shape algorithm.⁴⁵ ROCS treats atoms as a Gaussian function, and thus the overlaps between two (or more) atoms are also Gaussian functions. This algorithm implemented in ROCS speeds up the 3D shape-based calculations, as it involves calculating the maximal intersection of the volumes of two molecules.

For both compounds, 100 conformations were generated with Omega 2.3.2 software from OpenEye Scientific Software (www.eyesopen.com) and were compared to up to 100 conformations of each compound in the NCI and eMolecules databases using ROCS (version 3.0.0).⁴⁶ (The number of conformers generated for some rigid molecules in the database was less than 100.) Shape-based comparisons were quantified using two different metrics: 3D similarities, as quantified by the shape Tanimoto coefficient,⁴⁷ and 3D chemistry alignment, as quantified by the color score.⁴⁸ Chemistry alignment is specified by the color force field (implicit Mills–Dean⁴⁸) and accounts for the positioning of hydrogen bond donors, hydrogen bond acceptors, anions, cations, hydrophobic groups,

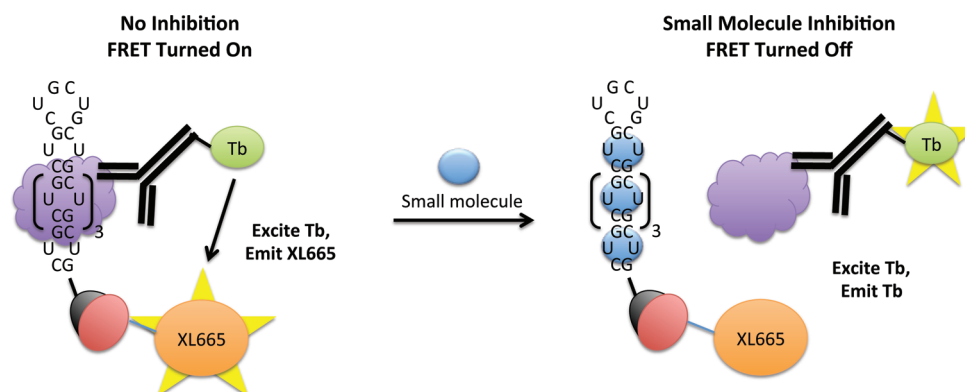


Figure 2. Schematic of the qTR-FRET assay used to determine the potencies of compounds for disrupting the $r(\text{CUG})_{12}$ -MBNL1 interaction. The $r(\text{CUG})_{12}$ oligonucleotide is labeled with a 5'-biotin, while MBNL1 contains a His₆ tag. (Left) In the absence of inhibitor, MBNL1 binds to $r(\text{CUG})_{12}$. Binding is quantified by using two antibodies that form a FRET pair—an anti-His6 antibody labeled with Tb that binds to MBNL1 and streptavidin labeled with XL665 that binds to $r(\text{CUG})_{12}$. The two fluorophores are within close enough proximity to form a FRET pair. Tb is excited at 345 nm; the resulting emission (~ 545 nm) excites XL665, which emits at 665 nm. (Right) In the presence of inhibitor, the $r(\text{CUG})_{12}$ -MBNL1 interaction is disrupted, and two fluorophores are not within close enough proximity to form a FRET pair. Therefore, emission is only observed at 545 nm (due to Tb). XL665 emission is not observed.

Table 1. IC₅₀'s for Displacement of MBNL1 from rCUG Repeats and Degree of Similarity to the Query Molecule (TanimotoCombo Score)^a

pentamidine-like			Hoechst-like		
small molecule	TanimotoCombo score	IC ₅₀ (μM)	small molecule	TanimotoCombo score	IC ₅₀ (μM)
pentamidine	—	>1000	Hoechst 33258	—	>1000
P1	1.45	10	H1	1.63	50
P2	1.47	50	H2	1.21	60
P3	1.30	60	H3	1.13	125
P4	1.13	200	H4	1.12	200
P5	1.36	250	H5	1.04	300
P6	1.33	375	H6	1.13	375
P7	1.07	375	H7	1.15	500
P8	1.55	1000	H8	1.03	500
			H9	1.08	500

^aThe error in the IC₅₀ measurements is $\pm 10\%$.

and rings. Complete overlap for either shape or color (chemistry alignment) is assigned a score of “1”, while no overlap is assigned a score of “0”. The molecules in the databases were then ranked on the basis of the “Tanimoto-Combo” score (sum of the shape Tanimoto coefficient and the color score; range = 0–2).

Since the compounds are similar to either Hoechst 33258 or pentamidine, it is likely that the compounds have similar binding preferences for RNA internal loops.⁴⁹ A subset of ~ 40 compounds was chosen for small molecules identified to be most similar to pentamidine; another subset of ~ 40 compounds was chosen for small molecules identified to be similar to Hoechst 33258 (Table S-3). These subsets were selected by visual inspection of the top 500 compounds to allow for maximal chemical diversity and their availability from the NCI or eMolecules repositories.

Identification of Inhibitors Using Quantitative Time-Resolved Fluorescence Resonance Energy Transfer (qTR-FRET). In order to screen the ligands identified via chemical similarity searching for disrupting the $r(\text{CUG})_6$ -MBNL1 complex, a qTR-FRET assay was used.^{50–52} A schematic of the assay is shown in Figure 2. Briefly, 5'-biotinylated $r(\text{CUG})_{12}$ and MBNL1-His₆ are pre-equilibrated, and then the compound of interest is added. Next, streptavidin-

XL665 (binds to the biotinylated RNA oligonucleotide) and Tb-Anti-His₆ (binds to MBNL1) are added. If the compound does not disrupt the $r(\text{CUG})_{12}$ -MBNL1 interaction, then XL665 and Tb are within close enough proximity to form a FRET pair, and the TR-FRET can be measured. TR-FRET is not observed if the compound inhibits formation of the $r(\text{CUG})_{12}$ -MBNL1 complex. It should be noted that the RNA-protein complex is preformed prior to addition of the compound of interest. Therefore, in order to be scored as an active compound, the small molecule must displace MBNL1 from the RNA.

We identified 17 compounds from the qTR-FRET screening assay that inhibited $\geq 85\%$ of $r(\text{CUG})_{12}$ -MBNL1 complex formation at 1 mM (Figure 1 and Table S-3). Interestingly, pentamidine and Hoechst only inhibit $\sim 10\%$ of $r(\text{CUG})_{12}$ -MBNL1 complex formation at 1 mM. The active compounds were then purified by HPLC, and the IC₅₀'s were measured (Table 1). The IC₅₀'s for the pentamidine-like compounds range from 10 to 1000 μM, while the IC₅₀'s for the Hoechst-like compounds range from 50 to 500 μM. Note that in 2D shape comparison the compounds are chemically quite distinct, but they show excellent shape similarity and functional group similarity as quantified by the combo score (Table 1). The best hits (P1, P2, P3, H1, and H2), which have IC₅₀'s ≤ 60 μM, were

structurally analyzed to determine an active chemotype. Each structure has two basic nitrogen atoms that are separated by similar distances, 15.1–18.0 Å (Figure 3).

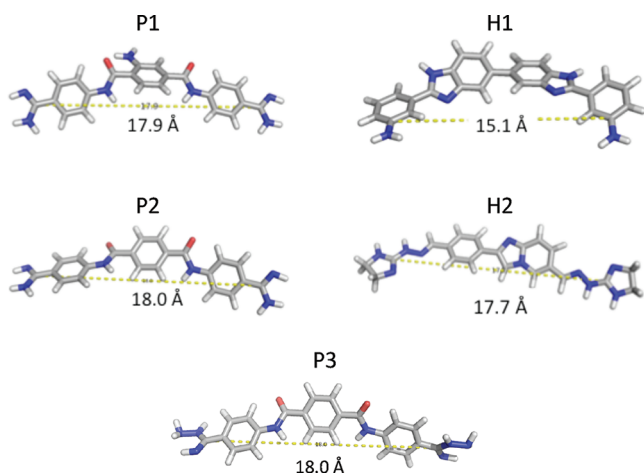


Figure 3. Structural analysis of the five most potent compounds that inhibit formation of the r(CUG)₁₂-MBNL1 complex using the TR-FRET assay depicted in Figure 2. Each structure has a similar distance between two carbon atoms that display a basic nitrogen.

Specificity of the Small Molecules for the DM1 Motif.

It is important that the small molecules that inhibit the rCUG-MBNL1 interaction show some level of specificity for the DM1 motif, 5'CUG/3'GUC. To estimate specificity, competition dialysis was employed. In these experiment, RNAs displaying the DM1 motif, a fully paired RNA, RNAs displaying other 1×1 nucleotide internal loops, an oligonucleotide mimic of the human aminoacyl tRNA site (A-site), and an oligonucleotide mimic of the cardiac troponin T (cTNT) pre-mRNA were used (Figure 4). The human A-site mimic was used because it is a likely cellular bystander RNA in mammalian cells and because it contains a 1×1 nucleotide UU internal loop motif. Furthermore, the human A-site is accessible for small-molecule binding in the context of the ribosome,^{53–55} and it is a highly abundant cellular RNA.⁵⁶ cTNT pre-mRNA is a natural substrate for MBNL1.²¹ It was used in order to determine if the small molecules might inhibit splicing of endogenous genes due to promiscuous binding. Compounds P1, P3, H1, and H2 were investigated; the spectral properties of P2 prevented study by competition dialysis, as the wavelengths at which it absorbs overlap with those of RNA.

First, the specificities of the compounds for the DM1 motif over a fully paired RNA and RNAs displaying other 1×1 nucleotide internal loops were investigated (Figure 5A). The most selective compound is P1, as it binds the DM1 motif preferentially over all other RNAs investigated. In contrast, P3 binds similarly to RNAs containing 5'C₂CG/3'G₂AC, 5'C₂GG/3'G₂AC, 5'C₂CG/3'G₂UC, 5'C₂AG/3'G₂CC, and the DM1 motif. Although the greatest amount of binding for H1 is observed to the DM1 motif, significant binding is also observed to 5'CUG/3'G₂CC, 5'C₂GG/3'G₂GC, and 5'C₂AG/3'G₂AC. H2 binding preferences are 5'C₂GG/3'G₂GC > 5'C₂CG/3'G₂UC ≈ 5'CUG/3'G₂UC ≈ 5'C₂GG/3'G₂AC.

Next, we investigated whether the amount of binding of P1 and H1 increased as a function of the number of DM1 motifs present in an RNA (Figure 5B). Thus, competition dialysis experiments were completed for RNAs containing 1–6 copies

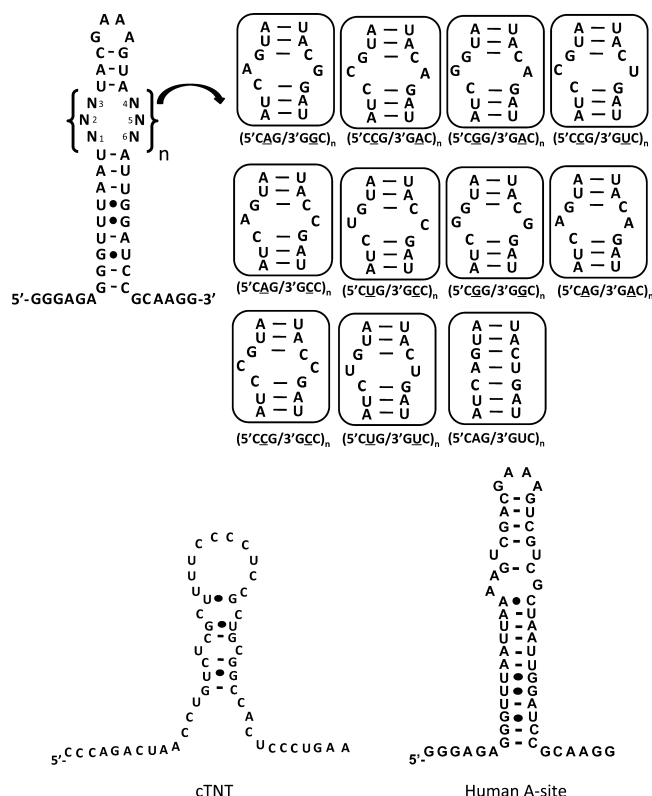


Figure 4. Secondary structures of the RNAs used to determine the specificities of P1, P3, H1, and H2, which are four of the most potent inhibitors of the r(CUG)₁₂-MBNL1 complex. RNAs containing only one copy of a motif are referred to as 5'C₂XG/3'G₂XC.

of 5'CUG/3'GUC, an oligonucleotide mimic of the human A-site, an oligonucleotide mimic of the cTNT pre-mRNA, and MBNL1 (Figure 4). MBNL1 was included in competition dialysis experiments since significant binding of the small molecules to MBNL1 could inhibit its normal function. In both cases, increased binding of the ligand is observed as the number of 5'CUG/3'GUC motifs present in the RNA increases (Figure 5B). The binding of H1 appears to be approximately stoichiometric, in good agreement with a previous report for another Hoechst derivative.⁴⁰ Moreover, H1 binds preferentially to RNAs with multiple DM1 motifs over MBNL1 and oligonucleotide mimics of the human A-site and cTNT pre-mRNA. In contrast, P1 does not bind stoichiometrically as the number of DM1 motifs increases from one to six. P1 also binds similarly to the human A-site and RNAs containing three or more DM1 motifs, and significant binding is observed to the mimic of the cTNT pre-mRNA (Figure 5B).

The affinities of H1 for an RNA containing one 5'CUG/3'GUC (DM1) motif and a fully paired RNA (Figure 4) were determined by fluorescence anisotropy. In good agreement with our competition dialysis results (Figure 5), H1 binds approximately 2-fold more tightly to the RNA with the DM1 motif (70 ± 32 nM) than to the fully paired RNA (190 ± 61 nM) (Supporting Information, Figure S-25).

A Bichromatic Reporter System and Flow Cytometry Analysis To Assess Bioactivity. To investigate whether P1, P2, P3, H1, and H2 are biologically active, we performed an initial cell-based screen using a modified bichromatic reporter⁵⁷ of alternative splicing (Figure 6A). The reporter contains human muscleblind exon 5 and adjacent introns. The splicing of this reporter is controlled by MBNL1 itself, through binding

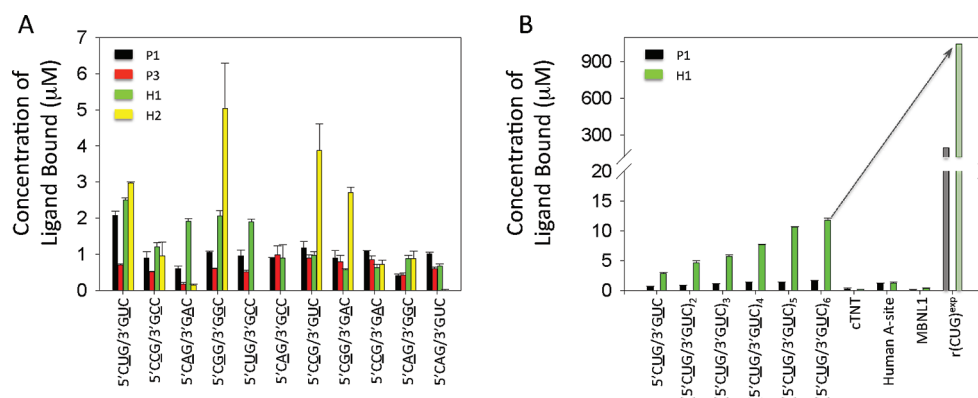


Figure 5. Results of competition dialysis experiments used to determine the specificities of a subset of the most potent compounds identified from the qTR-FRET assay. Not all of the compounds could be further investigated due to their spectroscopic properties; that is, their absorbance spectra overlapped with the absorbance from the RNAs or protein. (A) The specificities of four compounds were investigated by competition dialysis. Each compound was incubated with the 11 RNAs shown in the top panel of Figure 4. The concentration of bound ligand was determined using UV spectroscopy. P1 and H1 were the most promising ligands, as they bind an RNA containing 5'CUG/3'GUC more than the other RNAs. (B) The specificities of P1 and H1 were further investigated by competition dialysis with RNAs containing one to six copies of the DM1 motif (5'CUG/3'GUC), oligonucleotide mimics of the human A-site and the cTNT pre-mRNA, and MBNL1. The human A-site RNA and the cTNT pre-mRNA are representative bystander RNAs. The binding of H1 and P1 to r(CUG)^{exp} (shaded bars) was extrapolated on the basis of the presence of 479 copies of the 5'CUG/3'GUC motif in the DM1 cellular model system used in these studies.

and repression close to the 3' splice site. The reporter was designed such that exon 5 exclusion leads to translation of the DsRed reading frame, and exon 5 inclusion leads to a read-through of the +2 reading frame of DsRed, followed by subsequent translation of the EGFP reading frame. Splicing behavior was assessed by flow cytometry, where the number of cells expressing DsRed and EGFP at various levels can be divided into several quadrants (Figure 6B).

The behavior of the splicing reporter is consistent with that of endogenous MBNL1 exon 5, as observed upon transfection into HeLa cells. When transfected alone, ~55% of cells express DsRed or a combination of DsRed and EGFP. Upon co-transfection with a plasmid encoding mouse MBNL1 coding sequence, the percentage of cells that express DsRed or DsRed and EGFP increases to ~70% (Figure 6C,D). This is consistent with increased levels of MBNL1 blocking inclusion of the test exon, leading to increased DsRed production relative to EGFP. Likewise, when the reporter is co-transfected with a mini-gene containing 960 CUG repeats in the *DMPK* context (DT960),²¹ ~0% of cells express DsRed (Figure 6C,D). This is consistent with sequestration of endogenous MBNL1 by CUG repeats, leading to exon inclusion and increased EGFP production relative to DsRed production. Taken together, these results confirm that this bichromatic splicing reporter, which contains MBNL1 exon 5 as a test exon, can be used as a sensitive method for assessing cellular perturbations that affect MBNL1 activity.

To assess the biological activity of our compounds, we co-transfected our bichromatic splicing reporter, along with DT960, into three different cell lines. These lines include two different C2C12 mouse myoblast lines; one is a subclone of the original line (obtained from ATCC), and the other is the same subclone containing a stably integrated control shRNA hairpin that has been designed to not target any endogenous transcripts. After co-transfection of 250 ng of the reporter and 25 ng of DT960, the cells were treated with 20 μM P1, P2, P3, H1, or H2. Two days later, cells were analyzed by flow cytometry.

Similar results were observed in both C2C12 lines (Figure 6E,F). As expected, co-transfection with DT960 reduces the

fraction of cells that express DsRed. In the presence of DT960, compounds P1, P2, P3, and H2 led to a further reduction in the fraction of cells that express DsRed as compared to untreated cells containing DT960. In contrast, H1 led to a modest increase in the fraction of cells expressing DsRed, suggesting it can block or rescue the effects of CUG repeats on endogenous MBNL1 activity.

As an additional control, the effect of H1 on the bichromatic reporter in the absence of DT960 was also tested in C2C12 and HeLa (Figure 6G,H). Addition of 20 μM H1 to cells in the absence of DT960 led to a slight decrease in the fraction of cells expressing DsRed. However, addition of 20 μM H1 in the presence of DT960 led to a modest rescue relative to untreated cells in the presence of DT960, as evidenced by increased fractions of C2C12 and HeLa cells expressing DsRed (Figure 6G,H). These results suggest that of all the compounds, H1 exhibits biological activity in a manner favorable to counteracting the downstream effects of CUG repeats in the context of DM1.

H1 Improves Splicing Defects in a DM1 Cell Culture Model.

Next, we determined if the five most potent compounds could improve splicing defects in a DM1 cellular model system³⁸ using a cTNT mini-gene.²¹ cTNT pre-mRNA is mis-spliced in myotonic dystrophy patients.^{21,58,59} In normal cells, MBNL1 binds upstream of exon 5 in the cTNT pre-mRNA and represses its inclusion.^{58,60} In the absence of rCUG repeats, approximately 65% of exon 5 is included in cTNT mRNA, while in the presence of rCUG repeats, approximately 90% of exon 5 is included (Figure 7A). HeLa cells were co-transfected with plasmids containing a DM1 mini-gene that encodes 960 CTG repeats in a 3'UTR²¹ and the cTNT pre-mRNA mini-gene.²¹ The compound of interest was then added at a final concentration of 500 μM in growth medium. No improvement in splicing was observed for P1, P2, P3, or H2 (Supporting Information, Figure S-23), in good agreement with a bichromatic splicing reporter (Figure 6).⁵⁷

In contrast, modest improvement of splicing is observed when the cells are treated with 500 μM H1 (Figure 7A). More significant improvement is observed when cells are treated with 1 mM and 2 mM H1, improving splicing patterns almost to

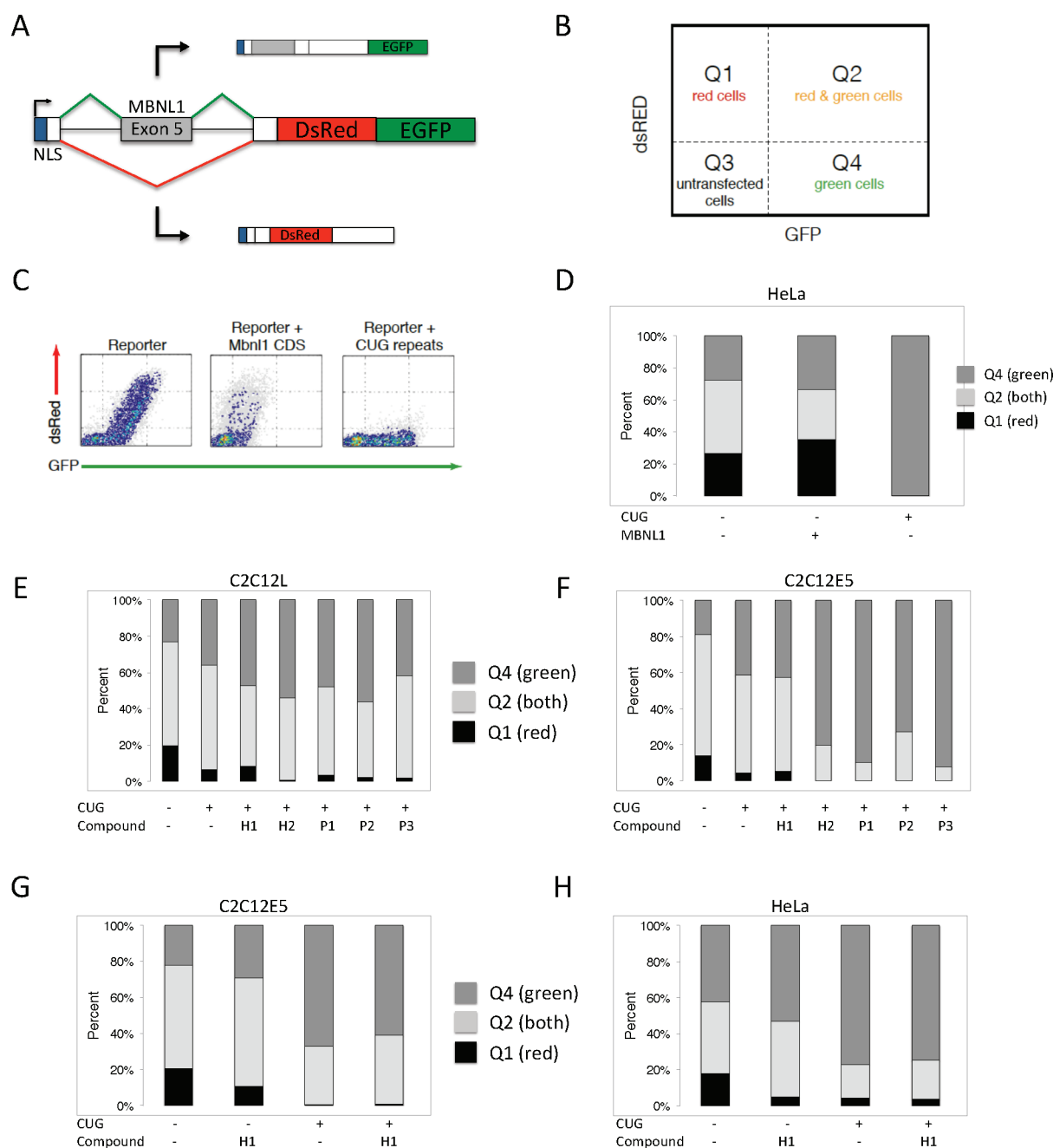


Figure 6. (A) Schematic of a bichromatic splicing reporter. The test region is human muscleblind exon 5 and adjacent introns, and replaces test exons in previous versions of the reporter.⁵⁷ Inclusion of the exon leads to EGFP expression, and exclusion leads to DsRed expression. (B) A simple method for quantitation of reporter behavior uses quadrants thresholded on EGFP and DsRed expression in cells. The fraction of cells in Q1, Q2, and Q4 relative to transfected cells (Q1 + Q2 + Q4) can be used as a metric for reporter behavior. (C) Representative flow cytometry plot of the reporter transfected alone, with MBNL1 coding sequence, or with 960 CUG repeats. The DsRed/EGFP ratio is responsive to MBNL1 activity. (D) Representative quantitation of reporter behavior in response to MBNL1 coding sequence or 960 CUG repeats, of which the former leads to increased DsRed expression, and the latter leads to increased EGFP expression. (E–H) Quantitation of reporter response to CUG repeats and compounds in combination. As illustrated in panels E and F, compound H1 exhibits the highest DsRed/EGFP ratio, relative to all other compounds in the presence of CUG repeats, in two different C2C12 cell subclones (C2C12L and C2C12E5). Panels G and H show instances in which compound H1 can partially rescue the effect of CUG repeats on reporter splicing patterns in both C2C12 and HeLa cells. Note that compound H1 alone, in the absence of CUG repeats, leads to a slight increase in EGFP expression relative to DsRed.

wild-type (WT). (The difference in inclusion percentage for WT cells (absence of $r(\text{CUG})^{\text{exp}}$) and $r(\text{CUG})^{\text{exp}}$ -expressing cells treated with 1 mM or 2 mM of H1 is not considered to be significant as determined by statistical analysis.) The difference in inclusion percentage for $r(\text{CUG})^{\text{exp}}$ -expressing cells that are untreated (Figure 7A, column 2) and treated with 1 mM or 2

mM of H1 is statistically significant. The two-tailed p -values are 0.0149 and 0.0192 for cells treated with 1 mM and 2 mM H1, respectively. Interestingly, Hoechst 33258 does not improve splicing defects in cTNT processing at these concentrations (Supporting Information, Figure S-24).

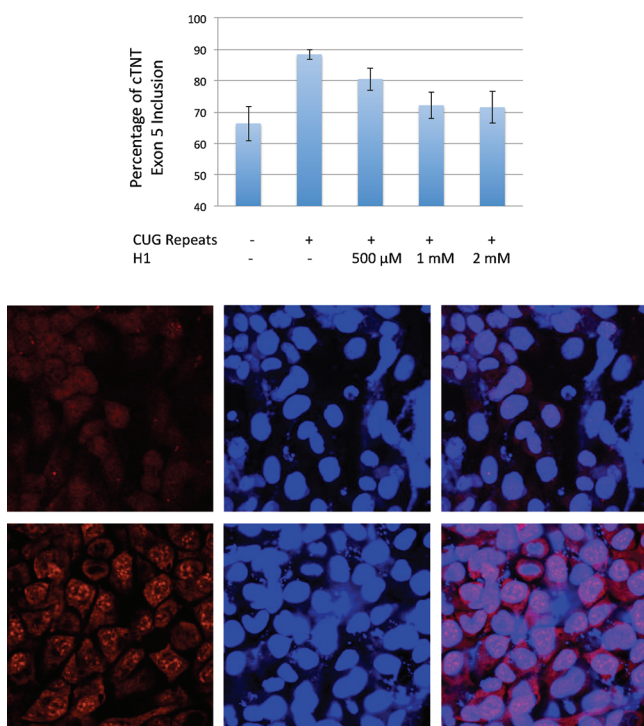


Figure 7. H1 improves splicing defects and disrupts nuclear foci in a DM1 cell culture model. (A) H1 improves defects in cTNT pre-mRNA splicing nearly to wild-type levels. The error bars indicate standard error. The difference in inclusion percentage for untreated cells that express r(CUG)^{exp} and treated cells (1 mM and 2 mM of H1) is statistically significant. The two-tailed *p*-values are 0.0149 and 0.0192 for cells treated with 1 mM and 2 mM H1, respectively. (B) Top, H1 disrupts formation of nuclear foci as determined by fluorescence *in situ* hybridization; bottom, untreated cells with multiple nuclear foci. The microscopic images from left to right are DY-547 fluorescence indicating the presence of CUG repeats, DAPI, and overlay of DY-547 and DAPI.

Control experiments were also completed in order to determine if H1 globally affects splicing. First, HeLa cells were co-transfected with plasmids containing a mini-gene with only five CTG repeats in the 3'UTR and the cTNT mini-gene.²¹ H1 does not affect cTNT splicing in the absence of CTG repeats (Supporting Information, Figure S-21). We also investigated whether H1 affects the splicing of pre-mRNAs whose splicing is not regulated by MBNL1 (Supporting Information, Figure S-22). A Pleckstrin-2 (*PLEKHH2*) mini-gene³⁸ was co-transfected with the DM1 mini-gene, and the cells were treated with H1. H1 does not affect the splicing of a *PLEKHH2* mini-gene at 2 mM. The splicing of endogenous genes tetratricopeptide repeat domain 8 (TTC8) and calcium/calmodulin-dependent protein kinase kinase 2 (CAMKK2) also was not affected. Thus, H1 does not globally affect RNA splicing; rather, it affects the splicing of pre-mRNAs controlled by MBNL1.

The toxicities of the compounds were assessed by flow cytometry using standard forward and side scatter metrics and propidium iodide (PI) staining (Supporting Information, Figure S-26). PI stains DNA in cells that are still grossly intact but permeabilized; treatment of cells with DMSO results in a slight increase in the percentage of cells stained with PI. Briefly, HeLa cells were treated with 500 μ M P1, P2, P3, or H1, and their scatter metrics and PI staining were compared to those of cells treated with 2% DMSO and those grown in medium

alone. Notably, treatment with P1 and P2 yields a large number of observed events with low forward scatter area and height values, indicating that most observed events represent cell debris. Treatment of cells with P3 also leads to loss of cell integrity but to a lesser extent. Following H1 treatment, over half of the cells still remain within each gate, indicating that cell integrity is largely preserved. In summary, H1 is by far the least cytotoxic compound as compared to P1, P2, and P3 (Supporting Information, Figure S-26).

H1 Disrupts Formation of Nuclear Foci in a Cell Culture Model of DM1. Another hallmark of myotonic dystrophy is the formation of nuclear foci, which consist of expanded rCUG repeats and proteins including MBNL1.^{30,34,35,61} In order to determine if H1 is able to disrupt or prevent formation of nuclear foci, a fluorescence *in situ* hybridization (FISH) assay was used. HeLa cells were co-transfected with a plasmid encoding the DM1 mini-gene. After incubation with H1, the cells were fixed, permeabilized, and incubated with a DY547-labeled, 2'OMe oligonucleotide complementary to the rCUG repeats.³⁸ H1 decreases the percentage of cells with nuclear foci when the cells are dosed with 2 mM and 1 mM compound (Figure 7B) but not with 500 μ M.

H1 Improves Splicing Defects in a Mouse Model of DM1. A mouse model of DM1 has been reported in which 250 rCUG repeats are expressed using an actin promoter (human skeletal actin long repeat, HSA^{LR}).²² The presence of the repeats causes the mis-splicing of the chloride ion channel (chloride channel 1, skeletal muscle, *Cln1*) and the sarcoplasmic/endoplasmic reticulum calcium ATPase 1 (*Serca1/Atp2a1*) pre-mRNAs. Normal adult mice have a *Cln1* exon 7a exclusion rate of $96 \pm 0.2\%$; DM1 mice have an exclusion rate of $54 \pm 1.4\%$. When DM1 mice are dosed with 80 mg/kg and 100 mg/kg, the exclusion rate is partially rescued to $66 \pm 0.6\%$ and $69 \pm 1.4\%$, respectively (Figure 8). These improvements in splicing are statistically significant as determined by a *t* test. (The two-tailed *p*-values are 0.0066 for treatment with 80 mg/kg of H1 and 0.0016 for treatment with 100 mg/kg of H1.) *Serca1* mis-splicing is also partially rescued. In normal adult mice, the inclusion rate for exon 22 is $99.8 \pm 0.1\%$, while the inclusion rate in the HSA^{LR} line is only $30 \pm 0.6\%$. Both dosages of H1, 80 mg/kg and 100 mg/kg, rescue splicing similarly with inclusion rates of $41 \pm 4.0\%$ and $42 \pm 3.0\%$, respectively (Figure 8). The improvement in splicing is statistically significant when the mice are treated with 100 mg/kg of H1. (The two-tailed *p*-values are 0.0522 for treatment with 80 mg/kg of H1 and 0.0176 for treatment with 100 mg/kg of H1.)

Selectivity of H1 Binding to DM1 RNA. Because H1 improves splicing defects in cellular and animal models of DM1 and exhibits little toxicity, it must have at least modest selectivity *in vivo*. There is little difference in binding affinity or selectivity of H1 for an RNA with a single copy of the DM1 motif and a fully paired RNA or a mimic of the human A-site (~ 2 -fold). However, the selectivity of H1 for RNAs containing 5'CUG/3'GUC improves as the number of repeats increases (Figure 5). That is, there is only a small difference in the binding of H1 to an RNA with a single motif and a fully paired RNA (Figure 5A), while an ~ 12 -fold difference in binding is observed between an RNA with six DM1 motifs ((5'CUG/3'GUC)₆) and a fully paired RNA (Figure 5). Thus, H1 could exhibit some level of specificity for r(CUG)^{exp} *in vivo* despite the presence of highly expressed bystander RNAs that also

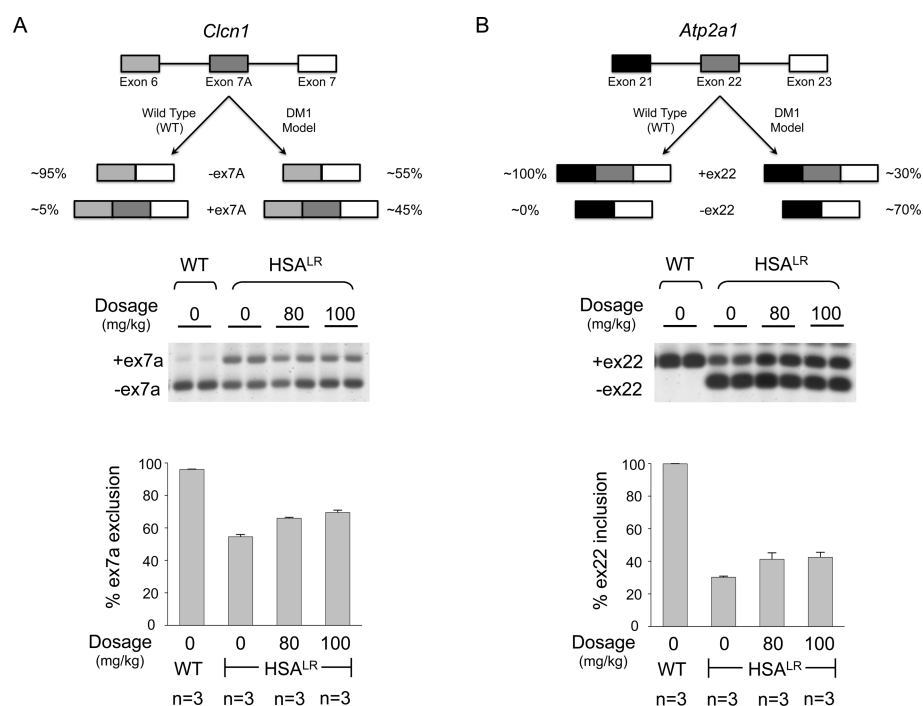


Figure 8. H1 improves splicing defects in the muscle-specific chloride ion channel (*Clcn1*) and sarco(endo)plasmic reticulum ATPase (*Atp2a1* / *Serca1*) pre-mRNAs in a DM1 mouse model. The DM1 mouse model expresses the human skeletal actin (HSA) transgene containing 250 CTG repeats (HSA^{LR}; where LR indicates “long repeats”). WT, or wild-type, refers to FVB mice.²² (A) Top, schematic of *Clcn1* alternative splicing in WT and DM1 mice; bottom, analysis of *Clcn1* alternative splicing by reverse transcription-polymerase chain reaction (RT-PCR) when mice are treated with H1, including a representative gel image and a plot of the corresponding data. The two-tailed *p*-values are 0.0066 for treatment with 80 mg/kg of H1 and 0.0016 for treatment with 100 mg/kg of H1. (B) Top, schematic of *Atp2a1* (*Serca1*) alternative splicing in WT and DM1 mice; bottom, analysis of *Atp2a1* alternative splicing by RT-PCR when mice are treated with H1, including a representative gel image and a plot of the corresponding data. The two-tailed *p*-values are 0.0522 for treatment with 80 mg/kg of H1 and 0.0176 for treatment with 100 mg/kg of H1.

contain the DM1 motif or a similar one. For example, the human A-site (Figure 4) is a highly abundant transcript that contains a single 5'GUC/3'CUG motif (two CUG repeats). At a first consideration, it would be assumed that it would be the most occupied binding site *in vivo*. However, DM1 is caused by hundreds of copies of the 5'CUG/3'GUC motif. In our cellular model system, r(CUG)^{exp} contains 479 copies of the 5'CUG/3'GUC motif ((CUG)₉₆₀). Thus, the selectivity of H1 for r(CUG)^{exp} over the A-site could be extrapolated from competition dialysis experiments by normalizing for the number of repeats present *in vivo*, or 479 times greater than the selectivity of the monomer (~2-fold) (shaded bars in Figure 5B).

Implications. Most RNAs that contribute to disease are unexploited as drug targets. This is generally thought to be due to a lack of information about the privileged scaffolds that specifically target RNA. In this study, a lead molecule was identified by analysis of an RNA motif–ligand database. Previous studies have shown that Hoechst 33258⁴⁴ and a derivative thereof⁴⁰ bind the regularly repeating 5'CUG/3'GUC motif that is present in DM1 RNA. By using chemical similarity searching, a series of related compounds that have improved *in vitro* potencies were identified. Importantly, one compound, H1, is specific for RNAs containing multiple 5'CUG/3'GUC motifs over mimics of a highly abundant, accessible RNA target (the human A-site) and a natural MBNL1 substrate (cTNT pre-mRNA). The compound improves splicing defects in cell and animal models and disrupts formation of nuclear foci in cells. Fortuitously, H1 was identified among the ~80 compounds that were hand-selected from ~500 virtual

screening hits with known activities. Additional compounds could have been screened if required.

Perhaps bioactive small molecules that target other RNAs could be discovered using an approach similar to the one described herein. Lead small molecules that are not bioactive due to poor cellular permeability, toxicity, etc. could be optimized via chemical similarity searching and then tested *in vitro* or *in vivo*. Two key developments bolster the likelihood of the applicability of the method: (i) a clearer understanding of the RNA motifs that bind small molecules and the chemical scaffolds that bind RNA and (ii) annotation of the RNA motifs present in RNAs that cause disease, including the HIV genome. By leveraging information in these two areas with compound optimization as described herein, bioactive small molecules that target other RNAs could be identified.

SUMMARY AND CONCLUSIONS

A computational approach was used to identify compounds similar to known *in vitro* inhibitors of a toxic RNA–protein interaction that have improved potencies and bioactivity. A bioactive, nontoxic ligand was identified that is similar to the Hoechst query molecule. Since Hoechst 33258 was identified as a DM1 RNA binder through analysis of an RNA motif–ligand database, these studies suggest that the database can provide lead ligands targeting RNA that can be further improved via computational screening. Furthermore, the H1 ligand module can be further improved for targeting the DM1 RNA by using a modular assembly strategy, which has been shown to improve the *in vitro* potency of compounds targeting the DM1 RNA by

orders of magnitude.⁴⁰ This approach could be generally applicable to any RNA of interest.

MATERIALS AND METHODS

Chemical Similarity Searching. Chemical similarity searching was performed on Dell P4 (64-bit) Linux clusters with 32 Xeon processors using Omega 2.3.2 (version 2.02) and ROCS (version 3.0.0) software from OpenEye Scientific Software (www.eyesopen.com). As a starting point for the virtual screen, Chem3D (Cambridge software) was used to energy-minimize (MMFF94 force field) a 3D conformer of pentamidine and Hoechst 33258. Omega 2.3.2 (version 2.02) was used to generate 100 conformers of pentamidine and Hoechst 33258, which were submitted as neutral molecules without any explicit charge. Then, up to 100 conformers of each molecule in the NCI and eMolecules database were generated. (The number of conformers generated for some rigid molecules in the database was less than 100.) The 500 compounds that were the most similar to pentamidine and the 500 compounds that were most similar to Hoechst 33258, as determined by the TanimotoCombo scores, were output in rank order as potential hits.^{45–47} Of these compounds, 88 were obtained (80 from NCI and 8 from ChemDiv (identified from eMolecules database)), and 14 were eliminated from screening due to their insolubility in DMSO or H₂O. A complete list of the compounds screened is available in the Supporting Information (Table S-3).

Three-dimensional shape comparisons, both the shape Tanimoto coefficients and color scores (chemistry alignment), were completed using Rapid Overlay of Chemical Structure (ROCS, version 3.0.0) from the OpenEye software package. The chemistry alignment overlap (color score) was calculated by using the color force field (explicit or implicit Mills–Dean as reported in the literature⁴⁸). The Tanimoto-Combo score is the sum of the shape Tanimoto coefficient and the color score.

Mass Spectroscopy and HPLC Purification. Mass spectra were collected on a Varian 500 MS spectrometer equipped with Varian Prostar Autosampler 410 and/or on an ABI 4800 MALDI-TOF spectrometer.

HPLC purifications were completed on a Waters 1525 binary HPLC pump equipped with a Waters 2487 dual absorbance detector system. Compounds were purified using a gradient of 5 mL/min, and a linear gradient of 0% to 100% B in A over 55, 50, or 46 min (A = water + 0.1% trifluoroacetic acid (TFA) (v/v); B = MeOH + 0.1% TFA (v/v)).

The purities of compounds were determined by analytical HPLC using a Waters 1525 binary HPLC pump equipped with Waters 2487 dual λ absorbance detector system and the following conditions: a Waters Symmetry C8 5 μ m 4.6 \times 150 mm column, room temperature, a flow rate of 2.4 mL/min, and a linear gradient of 0% to 100% B in A over 45 min.

Oligonucleotide Preparation and Purification. The RNA used in qTR-FRET assays (5'-biotinylated (CUG)₁₂) was purchased from Dharmacon. The 2-O-[bis[2-(acetoxy)ethoxy]methyl] (ACE) protecting groups were cleaved using Dharmacon's deprotection buffer. The sample was lyophilized, dissolved in Milli-Q water, and desalted using a PD-10 gel filtration column (GE Healthcare). RNAs used in competition dialysis experiments were prepared via runoff-transcription using synthetic DNA templates (Integrated DNA Technologies, Inc.) and a Stratagene RNAMaxx transcription kit. They were purified by denaturing polyacrylamide gel electrophoresis as previously described⁶² and dissolved in 1X competition dialysis buffer (8 mM NaH₂PO₄, 185 mM NaCl, and 1 mM EDTA; pH 7.2).

Oligonucleotide concentrations were determined by absorbance at 260 nm (90 °C for the RNA used in qTR-FRET assays; room temperature for RNAs used in competition dialysis) using a Beckman Coulter DU800 UV–vis spectrophotometer equipped with a Peltier temperature controller unit. Oligonucleotide extinction coefficients were determined using HyTher version 1.0 (Nicolas Peyret and John SantaLucia Jr., Wayne State University, Detroit, MI).^{63,64} The parameters used by HyTher were calculated using information on the extinction coefficients of nearest neighbors in RNA.⁶⁵

Quantitative Time-Resolved Fluorescence Resonance Energy Transfer (qTR-FRET) Assay. The qTR-FRET assay used to identify lead inhibitors of the r(CUG)₁₂-MBNL1 complex is based on PubChem BioAssay AID 2675 (Figure 2). Briefly, 5'-biotinylated r(CUG)₁₂ was folded in 1X folding buffer (20 mM 4-(2-hydroxyethyl)-1-piperazineethanesulfonic acid (HEPES), pH 7.5, 110 mM KCl, and 10 mM NaCl) by heating at 60 °C followed by slowly cooling to room temperature on the benchtop. The buffer was adjusted to 1X assay buffer (20 mM HEPES, pH 7.5, 110 mM KCl, 10 mM NaCl, 2 mM MgCl₂, 2 mM CaCl₂, 5 mM dithiothreitol, 0.1% bovine serum albumin (BSA), and 0.5% Tween-20), and MBNL1-His₆ was added. The final concentrations of RNA and MBNL1 were 80 nM and 60 nM, respectively. The sample was allowed to equilibrate at room temperature for 5 min, and then the compound of interest was added. After 15 min, streptavidin-XL665 (cisbio Bioassays) and anti-His₆-Tb (cisbio Bioassays) were added to final concentrations of 40 nM and 0.44 ng/ μ L, respectively, in a total of 10 μ L. The samples were incubated for 1 h at room temperature and then transferred to a well of a white 384-well plate. Time-resolved fluorescence was measured on a Molecular Devices SpectraMax M5 plate reader. Fluorescence was first measured using an excitation wavelength of 345 nm and an emission wavelength of 545 nm (fluorescence due to Tb). TR-FRET was then measured by using an excitation wavelength of 345 nm, an emission wavelength of 665 nm, a 200 μ s evolution time, and a 1500 μ s integration time. The ratio of fluorescence intensity of 545 and 665 nm as compared to the ratios in the absence of ligand and in the absence of RNA were used to determine IC₅₀'s.

Competition Dialysis. Pierce Slide-A-Lyzer MINI dialyzer units (Pierce Biotechnology, Inc.) were dialyzed against water for 24 h in order to ensure that the units did not leak. Competition dialysis was completed as previously described by Chaires.⁶⁶ Briefly, RNAs were folded by heating at 60 °C for 5 min, followed by slowly cooling to room temperature on the benchtop. Dialysis units containing 0.1 mL of 1.6 μ M RNA or MBNL1 were placed in 200 mL of 1 μ M ligand in 1X competition dialysis buffer. The samples were allowed to equilibrate with the dialysate by stirring the dialysate at 200 rpm for 24 h at room temperature (20–22 °C). Previous studies have shown that this is sufficient time for the sample to reach equilibrium.⁶⁶

At the end of the equilibration period, 67.5 μ L of each sample was carefully removed from the dialyzer unit and transferred to a microcentrifuge tube. To each sample, 7.5 μ L of 10% (w/v) sodium dodecyl sulfate (SDS) was added to give a final concentration of 1% (w/v) SDS, which is sufficient to dissociate the ligand. The SDS step was completed to ensure accurate determination of the concentration of bound ligand, as the spectroscopic properties of the bound ligand could be different from that of unbound. The total ligand concentration (C_t) within each dialysis unit was determined spectrophotometrically using an appropriate absorbance wavelength and extinction coefficient for each compound. Appropriate corrections were made for the small dilution resulting from the addition of the 10 μ L of SDS.

The free ligand concentration (C_f) was determined from an aliquot of the dialysate solution, which did not vary appreciable from the initial 1 μ M. The bound ligand concentration (C_b) was then determined using eq 1:

$$C_b = C_t - C_f \quad (1)$$

where C_b , C_v , and C_f are concentrations of bound, total, and free ligand, respectively.

Fluorescence Binding Assays. Dissociation constants were determined using an in-solution, fluorescence-based assay. RNA was annealed in 1X DNA buffer (8 mM Na₂PO₄, pH 7.0, 185 mM NaCl, 0.1 mM EDTA) at 60 °C for 5 min and allowed to slowly cool to room temperature. H1 was then added to a final concentration of 1000 nM. Serial dilutions of the RNA (1:2) were then completed in DNA buffer containing 1000 nM H1. The samples were incubated for 15 min at room temperature and then transferred to a well of a black 384-well plate. Anisotropy intensity was measured using a Molecular Devices SpectraMax M5 plate reader. The change in anisotropy as a

function of RNA concentration was fit to a standard one-site saturation ligand binding equation (eq 2):

$$y = \frac{B_{\max}x}{K_d + x} \quad (2)$$

where y is the observed anisotropy intensity, B_{\max} is the maximum anisotropy observed, x is the concentration of RNA, and K_d is the dissociation constant.

A Bichromatic Reporter System and Flow Cytometry Analysis To Assess Bioactivity. C2C12 and HeLa cell lines were maintained as monolayers in 1X DMEM supplemented with 20% or 10% fetal bovine serum (FBS), respectively. Cells were trypsinized from the surface and plated in 12-well plates in growth medium. While the cells were adhering to the surface, they were co-transfected with 25 ng of a plasmid encoding the DM1 mini-gene²¹ and 250 ng of a plasmid encoding a modified bichromatic fluorescent reporter of alternative splicing⁵⁷ using Transit (Mirus). (The bichromatic fluorescent reporter contains human MBNL1 exon 5 and adjacent introns in place of cTNT and its adjacent introns.) The compound of interest was then added (20 μ M). After 48 h, the cells were harvested by trypsinization. The trypsin was inactivated using growth medium, and the cells were immediately subjected to flow cytometry analysis using a BD LSR II.

Improvement of Splicing Defects in a Cell Culture Model Using RT-PCR. In order to determine if H1 improves splicing defects *in vivo*, a previously reported method was employed.³⁸ Briefly, HeLa cells were grown as monolayers in 12-well plates in growth medium (1X DMEM, 10% FBS, and 1X GlutaMax (Invitrogen)). After the cells reached 90–95% confluency, they were transfected with 800 ng of total plasmid using Lipofectamine 2000 reagent (Invitrogen) per the manufacturer's standard protocol. Equal amounts of a plasmid expressing a DM1 mini-gene with 960 CTG repeats²¹ and a mini-gene of interest (cTNT²¹ or PLEKHH2⁶⁰) were used. Approximately 5 h post-transfection, the transfection cocktail was removed and replaced with growth medium containing the compound of interest. After 16–24 h, the cells were trypsinized from the surface, and total RNA was harvested with a Qiagen RNeasy kit. An on-column DNA digestion was completed per the manufacturer's recommended protocol.

A sample of RNA was subjected to RT-PCR as previously described,⁶⁰ except 5 units of AMV reverse transcriptase from Life Sciences was used. Approximately 300 ng was reverse transcribed, and 150 ng was subjected to PCR using a radioactively labeled forward primer. RT-PCR products were observed after 25–30 cycles of 95 °C for 1 min, 55 °C for 1 min, 72 °C for 2 min, and a final extension at 72 °C for 10 min. The products were separated on a denaturing 5% polyacrylamide gel and imaged using a Typhoon phosphorimager.

Control experiments were also completed in which HeLa cells were transfected with a plasmid encoding a mini-gene with five CTG repeats in the 3'UTR or with a mini-gene that encodes a pre-mRNA whose splicing is not controlled by MBNL1 (PLEKHH2).⁶⁰ The effect of the compound on the splicing of endogenous mRNAs not under the control of MBNL1 (TTC8 and CAMKK2) was also determined as previously described.³⁸ Differences in alternative splicing were evaluated by a t test.

Disruption of Nuclear Foci Using Fluorescence *in Situ* Hybridization (FISH).³⁸ HeLa cells were grown as monolayers in Mat-Tak glass-bottomed, 96-well plates. After the cells reached 90–95% confluency, they were transfected with 100 ng of a plasmid encoding a DM1 mini-gene²¹ using Lipofectamine 2000 per the manufacturer's standard protocol. The transfection cocktail was removed 5 h post-transfection, and the compound of interest was added in growth medium.

After 16–24 h, the cells were washed with 1X Dulbecco's phosphate-buffered saline (DPBS) and fixed with 4% paraformaldehyde in 1X DPBS for 5 min at room temperature. After being washed with 1X DPBS, the cells were permeabilized with 1X DPBS + 0.1% Triton X-100 for 5 min at room temperature. The cells were washed with 1X DPBS + 0.1% Triton X-100 three times and then with 30%

formamide in 2X saline–sodium citrate (SSC) buffer (30 mM sodium citrate, pH 7.0, 300 mM NaCl) for 10 min at room temperature.

The cells were incubated in 1X FISH Buffer (30% formamide, 2X SSC Buffer, 66 μ g/mL bulk yeast tRNA, 2 μ g/mL BSA, 2 mM vanadyl complex (New England Bio Laboratories), and 1 ng/ μ L DY547-2'OMe-(CAGCAGCAGCAGCAGCAGC)) for 1.5 h at 37 °C. They were then washed with 30% formamide in 2X SSC for 30 min at 37 °C, 1X SSC for 30 min at room temperature, and 1X DPBS + 0.1% Triton X-100 for 5 min at room temperature. Finally, nuclei were stained by incubating the cells with 1 μ g/mL 4',6-diamidino-2-phenylindole (DAPI) for 5 min at room temperature. The cells were washed with 1X DPBS + 0.1% Triton X-100, and 100 μ L of 1X DPBS was added to each well. The cells were imaged using an Olympus FluoView 1000 confocal microscope at 60X magnification.

Treatment in Mice. All experimental procedures, mouse handling, and husbandry were completed in accordance with the Association for Assessment and Accreditation of Laboratory Animal Care. A mouse model for DM1, HSA^{LR} in line 20b,²² was used to investigate if H1 improves splicing defects in animals. HSA^{LR} mice express human skeletal actin RNA with 250 CUG repeats in the 3'UTR. Age- and gender-matched HSA^{LR} mice were injected intraperitoneally with 80 or 100 mg/kg H1 in 5% glucose or 5% glucose alone once per day for 7 days. Mice were sacrificed one day after the last injection, and the vastus muscle was obtained. RNA was extracted from the vastus tissue, and cDNA was synthesized as previously described.⁶⁷ PCR amplification was carried out for 22–24 cycles with the following primer pairs: *Cln1* forward 5'-TGAAGGAATACCTCACACT-CAAGG and reverse 5'-CACGGAACACAAAGGCACTG; *Atp2a1* forward 5'-GCTCATGGTCCTCAAGATCTCAC and reverse 5'-GGGTCAGTGCCTCAGCTTTG. The PCR products were separated by agarose gel electrophoresis, and the gel was stained with SYBR Green I (Invitrogen). The gel was scanned with a laser fluorimager (Typhoon, GE Healthcare), and the products were quantified using ImageQuant. Differences between two groups were evaluated by a t test.

■ ASSOCIATED CONTENT

● Supporting Information

Complete ref 14; complete list of all compounds tested in the original qTR-FRET screen (Table S-3); results of mass spectrometry for all compounds identified from the initial qTR-FRET screen (Tables S-1 and S-2); HPLC retention times and analytical HPLC chromatograms for all compounds identified from the initial qTR-FRET screen (Tables S-1 and S-2 and Figures S-4–S-20); details of the characterization and synthesis of H1 (Scheme S1, Figures S-1–S-3); representative autoradiograms of splicing outcomes as determined by RT-PCR (Figures S-21–S-24); representative binding curves (Figure S-25); and assessment of toxicity using flow cytometry (Figure S-26). This material is available free of charge via the Internet at <http://pubs.acs.org>.

■ AUTHOR INFORMATION

Corresponding Author

disney@scripps.edu

Author Contributions

[#]These authors contributed equally to this work.

Notes

The authors declare no competing financial interest.

■ ACKNOWLEDGMENTS

We dedicate this work to Douglas H. Turner on the occasion of his 65th birthday. We thank Sandro Matosevic for assistance with confocal microscopy, the URM Center for RNA Biology, the Rochester Wellstone Muscular Dystrophy Cooperative

Research Center, and Openeye and ChemAxon for providing free academic software. This work was funded by the National Institutes of Health (3R01GM079235-02S1 and 1R01GM079235-01A2 to M.D.D.; AR049077 to C.A.T.) and by The Scripps Research Institute. M.D.D. is a Camille & Henry Dreyfus New Faculty Awardee, a Camille & Henry Dreyfus Teacher-Scholar, and a Research Corporation Cottrell Scholar.

REFERENCES

- (1) Guthrie, C. *Science* **1991**, 253, 157.
- (2) Lee, R. C.; Ambros, V. *Science* **2001**, 294, 862.
- (3) Lau, N. C.; Lim, L. P.; Weinstein, E. G.; Bartel, D. P. *Science* **2001**, 294, 858.
- (4) Lagos-Quintana, M.; Rauhut, R.; Lendeckel, W.; Tuschl, T. *Science* **2001**, 294, 853.
- (5) Chabot, B. *Trends Genet.* **1996**, 12, 472.
- (6) Calin, G. A.; Croce, C. M. *Oncogene* **2006**, 25, 6202.
- (7) Caskey, C. T.; Pizzuti, A.; Fu, Y. H.; Fenwick, R. G. Jr.; Nelson, D. L.; Kuhl, D. P. *Science* **1992**, 256, 784.
- (8) Faustino, N. A.; Cooper, T. A. *Genes Dev.* **2003**, 17, 419.
- (9) Kalnina, Z.; Zayakin, P.; Silina, K.; Line, A. *Genes Chromosome Canc.* **2005**, 42, 342.
- (10) Caskey, C. T.; Pizzuti, A.; Fu, Y. H.; Fenwick, R. G. Jr.; Nelson, D. L. *Science* **1992**, 256, 784.
- (11) Ranum, L. P.; Cooper, T. A. *Annu. Rev. Neurosci.* **2006**, 29, 259.
- (12) Liquori, C. L.; Ricker, K.; Moseley, M. L.; Jacobsen, J. F.; Kress, W.; Naylor, S. L.; Day, J. W.; Ranum, L. P. *Science* **2001**, 293, 864.
- (13) Fu, Y. H.; Pizzuti, A.; Fenwick, R. G. Jr.; King, J.; Rajnarayan, S.; Dunne, P. W.; Dubel, J.; Nasser, G. A.; Ashizawa, T.; de Jong, P.; Wieringa, B.; Korneluk, R.; Perryman, M. B.; Epstein, H. F.; Caskey, C. T. *Science* **1992**, 255, 1256.
- (14) Brook, J. D.; et al. *Cell* **1992**, 68, 799.
- (15) Mykowska, A.; Sobczak, K.; Wojciechowska, M.; Kozlowski, P.; Krzyzosiak, W. J. *Nucleic Acids Res.* **2011**, 39, 8938.
- (16) Li, L. B.; Yu, Z.; Teng, X.; Bonini, N. M. *Nature* **2008**, 453, 1107.
- (17) Michlewski, G.; Krzyzosiak, W. J. *J. Mol. Biol.* **2004**, 340, 665.
- (18) Sellier, C.; Rau, F.; Liu, Y.; Tassone, F.; Hukema, R. K.; Gattoni, R.; Schneider, A.; Richard, S.; Willemsen, R.; Elliott, D. J.; Hagerman, P. J.; Charlet-Berguerand, N. *EMBO J.* **2010**, 29, 1248.
- (19) Kanadia, R. N.; Johnstone, K. A.; Mankodi, A.; Lungu, C.; Thornton, C. A.; Esson, D.; Timmers, A. M.; Hauswirth, W. W.; Swanson, M. S. *Science* **2003**, 302, 1978.
- (20) Kanadia, R. N.; Shin, J.; Yuan, Y.; Beattie, S. G.; Wheeler, T. M.; Thornton, C. A.; Swanson, M. S. *Proc. Natl. Acad. Sci. U.S.A.* **2006**, 103, 11748.
- (21) Philips, A. V.; Timchenko, L. T.; Cooper, T. A. *Science* **1998**, 280, 737.
- (22) Mankodi, A.; Logigian, E.; Callahan, L.; McClain, C.; White, R.; Henderson, D.; Krym, M.; Thornton, C. A. *Science* **2000**, 289, 1769.
- (23) Mankodi, A.; Takahashi, M. P.; Jiang, H.; Beck, C. L.; Bowers, W. J.; Moxley, R. T.; Cannon, S. C.; Thornton, C. A. *Mol. Cell* **2002**, 10, 35.
- (24) Paul, S.; Dansithong, W.; Kim, D.; Rossi, J.; Webster, N. J.; Comai, L.; Reddy, S. *EMBO J.* **2006**, 25, 4271.
- (25) Dansithong, W.; Paul, S.; Comai, L.; Reddy, S. J. *Biol. Chem.* **2005**, 280, 5773.
- (26) Savkur, R. S.; Philips, A. V.; Cooper, T. A. *Nat. Genet.* **2001**, 29, 40.
- (27) Hino, S.; Kondo, S.; Sekiya, H.; Saito, A.; Kanemoto, S.; Murakami, T.; Chihara, K.; Aoki, Y.; Nakamori, M.; Takahashi, M. P.; Imaizumi, K. *Hum. Mol. Genet.* **2007**, 16, 2834.
- (28) Kimura, T.; Nakamori, M.; Lueck, J. D.; Pouliquin, P.; Aoike, F.; Fujimura, H.; Dirksen, R. T.; Takahashi, M. P.; Dulhunty, A. F.; Sakoda, S. *Hum. Mol. Genet.* **2005**, 14, 2189.
- (29) Timchenko, N. A.; Cai, Z. J.; Welm, A. L.; Reddy, S.; Ashizawa, T.; Timchenko, L. T. *J. Biol. Chem.* **2001**, 276, 7820.
- (30) Fardaei, M.; Rogers, M. T.; Thorpe, H. M.; Larkin, K.; Hamshire, M. G.; Harper, P. S.; Brook, J. D. *Hum. Mol. Genet.* **2002**, 11, 805.
- (31) Ho, T. H.; Savkur, R. S.; Poulos, M. G.; Mancini, M. A.; Swanson, M. S.; Cooper, T. A. *J. Cell. Sci.* **2005**, 118, 2923.
- (32) Jiang, H.; Mankodi, A.; Swanson, M. S.; Moxley, R. T.; Thornton, C. A. *Hum. Mol. Genet.* **2004**, 13, 3079.
- (33) Mankodi, A.; Lin, X.; Blaxall, B. C.; Swanson, M. S.; Thornton, C. A. *Circ. Res.* **2005**, 97, 1152.
- (34) Mankodi, A.; Urbinati, C. R.; Yuan, Q. P.; Moxley, R. T.; Sansone, V.; Krym, M.; Henderson, D.; Schalling, M.; Swanson, M. S.; Thornton, C. A. *Hum. Mol. Genet.* **2001**, 10, 2165.
- (35) Miller, J. W.; Urbinati, C. R.; Teng-Umuay, P.; Stenberg, M. G.; Byrne, B. J.; Thornton, C. A.; Swanson, M. S. *EMBO J.* **2000**, 19, 4439.
- (36) Garcia-Lopez, A.; Llamusi, B.; Orzaez, M.; Perez-Paya, E.; Artero, R. D. *Proc. Natl. Acad. Sci. U.S.A.* **2011**, in press.
- (37) Mulders, S. A.; van den Broek, W. J.; Wheeler, T. M.; Croes, H. J.; van Kuik-Romeijn, P.; de Kimpe, S. J.; Furling, D.; Platenburg, G. J.; Gourdon, G.; Thornton, C. A.; Wieringa, B.; Wansink, D. G. *Proc. Natl. Acad. Sci. U.S.A.* **2009**, 106, 13915.
- (38) Warf, M. B.; Nakamori, M.; Matthys, C. M.; Thornton, C. A.; Berglund, J. A. *Proc. Natl. Acad. Sci. U.S.A.* **2009**, 106, 18551.
- (39) Wheeler, T. M.; Sobczak, K.; Lueck, J. D.; Osborne, R. J.; Lin, X.; Dirksen, R. T.; Thornton, C. A. *Science* **2009**, 325, 336.
- (40) Pushechnikov, A.; Lee, M. M.; Childs-Disney, J. L.; Sobczak, K.; French, J. M.; Thornton, C. A.; Disney, M. D. *J. Am. Chem. Soc.* **2009**, 131, 9767.
- (41) Lee, M. M.; Childs-Disney, J. L.; Pushechnikov, A.; French, J. M.; Sobczak, K.; Thornton, C. A.; Disney, M. D. *J. Am. Chem. Soc.* **2009**, 131, 17464.
- (42) Arambula, J. F.; Ramisetty, S. R.; Baranger, A. M.; Zimmerman, S. C. *Proc. Natl. Acad. Sci. U.S.A.* **2009**, 106, 16068.
- (43) Gareiss, P. C.; Sobczak, K.; McNaughton, B. R.; Palde, P. B.; Thornton, C. A.; Miller, B. L. *J. Am. Chem. Soc.* **2008**, 130, 16254.
- (44) Cho, J.; Hamasaki, K.; Rando, R. R. *Biochemistry* **1998**, 37, 4985.
- (45) Grant, J. A.; Gallardo, M. A.; Pickup, B. T. *J. Comput. Chem.* **1996**, 17, 1653.
- (46) Bostrom, J.; Greenwood, J. R.; Gottfries, J. J. *Mol. Graph. Model* **2003**, 21, 449.
- (47) Haigh, J. A.; Pickup, B. T.; Grant, J. A.; Nicholls, A. J. *Chem. Inf. Model* **2005**, 45, 673.
- (48) Mills, J. E.; Dean, P. M. *J. Comput. Aided Mol. Des.* **1996**, 10, 607.
- (49) Bostrom, J.; Hogner, A.; Schmitt, S. J. *Med. Chem.* **2006**, 49, 6716.
- (50) Boger, D. L.; Fink, B. E.; Brunette, S. R.; Tse, W. C.; Hedrick, M. P. *J. Am. Chem. Soc.* **2001**, 123, 5878.
- (51) Tse, W. C.; Boger, D. L. *Acc. Chem. Res.* **2004**, 37, 61.
- (52) Krishnamurthy, M.; Schirle, N. T.; Beal, P. A. *Bioorg. Med. Chem.* **2008**, 16, 8914.
- (53) Diop, D.; Chauvin, C.; Jean-Jean, O. C. R. *Biol.* **2007**, 330, 71.
- (54) Manuvakhova, M.; Keeling, K.; Bedwell, D. M. *RNA* **2000**, 6, 1044.
- (55) Nudelman, I.; Rebibo-Sabbah, A.; Cherniavsky, M.; Belakhov, V.; Hainrichson, M.; Chen, F.; Schacht, J.; Pilch, D. S.; Ben-Yosef, T.; Baasov, T. *J. Med. Chem.* **2009**, 52, 2836.
- (56) Berg, J. M.; Tymoczko, J. L.; Stryer, L. *Biochemistry*, 6th ed.; W.H. Freeman and Co.: New York, 2007.
- (57) Orengo, J. P.; Bundman, D.; Cooper, T. A. *Nucleic Acids Res.* **2006**, 34, e148.
- (58) Ho, T. H.; Charlet, B. N.; Poulos, M. G.; Singh, G.; Swanson, M. S.; Cooper, T. A. *EMBO J.* **2004**, 23, 3103.
- (59) Nezu, Y.; Kino, Y.; Sasagawa, N.; Nishino, I.; Ishiura, S. *Neuromuscul. Disord* **2007**, 17, 306.
- (60) Warf, M. B.; Berglund, J. A. *RNA* **2007**, 13, 2238.
- (61) Mankodi, A.; Teng-Umuay, P.; Krym, M.; Henderson, D.; Swanson, M.; Thornton, C. A. *Ann. Neurol.* **2003**, 54, 760.
- (62) Disney, M. D.; Childs-Disney, J. L. *Chembiochem* **2007**, 8, 649.

- (63) Peyret, N.; Seneviratne, P. A.; Allawi, H. T.; SantaLucia, J. Jr. *Biochemistry* **1999**, 38, 3468.
- (64) SantaLucia, J. *Proc. Natl. Acad. Sci. U.S.A.* **1998**, 95, 1460.
- (65) Puglisi, J. D.; Tinoco, I. Jr. *Methods Enzymol.* **1989**, 180, 304.
- (66) Chaires, J. B.; Ragazzon, P. A.; Garbett, N. C. *Curr. Protoc. Nucleic Acid Chem.* **2003**, 8.3.
- (67) Lin, X.; Miller, J. W.; Mankodi, A.; Kanadia, R. N.; Yuan, Y.; Moxley, R. T.; Swanson, M. S.; Thornton, C. A. *Hum. Mol. Genet.* **2006**, 15, 2087.